General and Comparative Endocrinology 277 (2019) 130–140

Contents lists available at ScienceDirect

General and Comparative Endocrinology

journal homepage: www.elsevier.com/locate/ygcen

Adamts9 is necessary for ovarian development in zebrafish

Nichole Jansch Carter, Zachary Adam Roach, Mckenzie Marie Byrnes, Yong Zhu*

Department of Biology, East Carolina University, Greenville 27858, NC, USA

ARTICLE INFO

Keywords:
Adamts9
Metalloproteinase
Ovarian development
Sexual development
Ovulation
Zebrafish

ABSTRACT

Expression of *adamts9* (A disintegrin and metalloprotease with thrombospondin type-1 motif, member 9) increases dramatically in the somatic cells surrounding oocytes during ovulation in vertebrates from zebrafish to human. However, the function of Adamts9 during ovulation has not been determined due to the embryonic lethality of knockouts in mice and *Drosophila*. To identify the role of Adamts9 during ovulation we generated knockout (*adamts9*$^{-/-}$) zebrafish using CRISPR/Cas9 and characterized the effects of the mutation. From 1047 fish generated by crossing *adamts9*$^{+/-}$ pairs, we found significantly fewer adult *adamts9*$^{-/-}$ fish (4%) than predicted by Mendelian ratios (25%). Of the mutants found, there was a significant male bias (82%). Only 3 female mutants were identified (7%), and they had small ovaries with few stage III and IV oocytes compared to wildtype (*wt*) counterparts of comparable size and age. Astoundingly, the remaining mutants (11%) did not appear to have normal testis or ovaries. Instead there was a pair of transparent, ovarian-like membranous shells that filled the abdominal cavity. Histological examination confirmed that shells were largely empty with no internal structure. Surprisingly, seminiferous tubules and various spermatocytes including mature spermatozoa were observed on the periphery of these transparent shells. No female or female like knockouts were observed to release eggs, and no ovulated oocytes were observed in histological sections. To our knowledge, this is the first report of an *adamts9* global knockout model in any adult vertebrates and the first description of how gonadal sex and structure are affected- highlighting the importance of Adamts9 during gonadal development and the value of zebrafish as a model organism.

1. Introduction

Expression changes of numerous metalloproteases during ovulation have been shown in various animals, yet specific proteases responsible for the terminal degradation of the follicular layers are still unknown (Handbook of Proteolytic Enzymes, 2012; Liu et al., 2017, 2018). Aberrant expression or mis-regulation of ADAMTS (A disintegrin and metalloprotease with thrombospondin type-1 motifs) and other matrix metalloproteases (MMPs) in the ovary can result in diseases like infertility, polycystic ovarian syndrome (PCOS), and cancer (Blelloch and Kimble, 1999; Huang et al., 2013; Handbook of Proteolytic Enzymes, 2012). By developing our understanding of how evolutionarily conserved metalloproteases degrade the follicular cells' basal membrane during the terminal stages of ovulation, researchers can find novel approaches to address diseases like PCOS, premature ovarian failure (POF) and infertility.

Adamts9 (A disintegrin and metalloprotease with thrombospondin type-1 motifs, member 9) is a cell-autonomous antiangiogenic metalloprotease with proteolytic and thrombospondin repeats that are highly conserved from *C. elegans* to humans (Somerville et al., 2003; Clark et al., 2000). The inactive Adamts9 protein is membrane bound until furin-cleavage releases into the extracellular space (Koo et al., 2006), where it digests large, hydrophilic extracellular matrix (ECM) proteoglycans like versican and aggrecan (Kern et al., 2010; McCulloch et al., 2009; Demircan et al., 2013). Bio-active fragments generated by Adamts9 are required for differentiation (Nandadasa et al., 2015) and cell death (McCulloch et al., 2009), throughout murine embryogenesis (Jungers et al., 2005; Enomoto et al., 2010).

Few reports are currently available on functions of Adamts9 in animals. Knockout of Adamts9 ortholog, GON-1 in *C. elegans* demonstrates its essential roles in germ cell migration and gonad formation (Blelloch and Kimble, 1999; Blelloch et al., 1999). Knockout of Adamts9 ortholog, Adamts-A, in *Drosophila* causes mis-migration of collective cells including germ cells (Ismat et al., 2013). Homozygous Adamts9 knockout mice die before gastrulation at E7 (Enomoto et al., 2010), which suggests essential roles of Adamts9 in the development, but also limits our understanding on the roles of Adamts9 during development and in adults. Currently, it is unknown whether Adamts9 plays any roles in the germ cell migration, maintenance, proliferation and gonad formation in any vertebrates.

* Corresponding author.
E-mail address: zhuy@ecu.edu (Y. Zhu).

https://doi.org/10.1016/j.ygcen.2019.04.003
Received 27 January 2019; Received in revised form 25 March 2019; Accepted 1 April 2019
Available online 02 April 2019

Zebrafish are a gonochoristic species (two distinct sexes) of teleost that utilize transitory hermaphroditism, where all juveniles first form undifferentiated ovaries containing primordial oocytes before undergoing apoptosis to develop as testes or as ovaries (Takahashi, 1977). In the early testis, primordial oocytes undergo a highly dynamic, poorly understood process which leaves cavities that become filled with clusters of cells reported to be testicular germ cells (Orban et al., 2009). The number of PGCs and primordial oocytes play an active role in determining zebrafish sex as embryos and larvae that have reduced numbers of germ cells (Rodríguez-Marí et al., 2010; Tzung et al., 2015), or none (Siegfried and Nüsslein-Volhard, 2008), result in male biased populations.

In mice, macaques and humans, the adamts9 transcript is cyclically induced by gonadotropins in ovarian follicular cells during the early stages of ovulation (Piprek et al., 2018; Peluffo et al., 2011; Rosewell et al., 2015), but its function in the adult ovary has not been previously studied due to the embryonic lethality of mouse and *Drosophila* knockouts (Jungers et al., 2005; Ismat et al., 2013). From previous analyses using RNA-seq and qPCR done by our lab on metalloprotease expression of mature oocytes of anovulatory zebrafish due to nuclear progestin receptor knockout (Pgr-KO), we found that *adamts9* had the most dramatically reduced expression (around 60-fold) compared to wildtype (*wt*) (Liu, et al., 2017, 2018). The conserved expression of adamts9 transcripts in the ovarian somatic cells of zebrafish, mice and humans, suggests that adamts9 plays a key role during ovulation. To determine the function of Adamts9 in the zebrafish ovary, we generated and characterized the phenotypes of *adamts9*$^{-/-}$ knockouts using CRISPR/Cas9.

2. Materials and methods

2.1. Animal husbandry

Wildtype (*wt*) *Danio rerio* (zebrafish), propagated in our lab are a Tübingen strain originally obtained from the Zebrafish International Resource Center, and are housed in automatically controlled rearing systems for zebrafish (Aquatic Habitats Z-Hab Duo systems, Florida, USA). Fish were bred in polycarbonate breeding tanks and reared in multiple 3-liter holding tanks with water temperature around 28.5 °C, salinity conductivity from 500 to 1200 μS, and pH around 7.2. Each 3-L holding tank houses an average of 30 fish per tank. The photoperiod was set to 14 h (hrs) of light (9:00 AM–11:00 PM) and 10 h of dark (11:00 PM–9:00 AM). Fish were fed commercial food with high protein content (Otohime B2, Reed Mariculture, CA, USA) until satiation and supplemented with freshly hatched artemia twice daily (Brine Shrimp Direct, UT, USA). East Carolina University's Institutional Animal Care and Use Committee (IACUC) has approved all experimental protocols.

2.2. CRISPR/Cas9 targets and sgRNA vectors

A CRISPR/Cas9 target site (TAGAAGTTGCAGTATTAATG) within the 7th exon of *adamts9*, spanning an AseI (ATTAAT) palindromic restriction enzyme (RE) site, and upstream of PAM (Protospacer Adjacent Motif) was selected. The targeted sequence was compared (using BLASTN) against the whole zebrafish genome and had low homology to other sites. A pair of oligonucleotides corresponding to the target was cloned into T7 gRNA (46759, Addgene) vector codon optimized for zebrafish using a modified protocol (Jao et al., 2013; Ran et al., 2013). Forward Primer sequence: AACACAAGGTGTAAAGCCCT; Reverse Primer Sequence: TTTGGACACTCAGGCCACAT (Fig. 1).

Briefly, the T7 gRNA vector (200 ng/μL) was linearized by sequential digestion, with BgII and SalI overnight at 37 °C. Digestion products were purified using Qiagen spin columns and DNA was eluted with DNase free water. The second digestion was done with BsmBI and DTT. The reaction was allowed to run overnight at 37 °C, and the enzyme was inactivated at 80 °C for 20 min, and then the DNA was gel purified. Linearized plasmid concentrations were quantified using Nanodrop 2000. Oligo sequences for desired gRNA forward and reverse sequences were ordered from Sigma and suspended in DNase free water to a final concentration of 100 μM. Oligos (sgRNA forward 1 μL, sgRNA reverse 1 μL) were phosphorylated using T4 polynucleotide kinase (PNK) and reactions were done using a thermocycler with the following settings: 37 °C for 30 min; 95 °C for 5 min; ramp down to 25 °C at −0.08 °C/s. After phosphorylation, annealed oligos were diluted (1:200) in order to be ligated into the linearized a pT7-gRNA vector. Diluted oligos, 2× rapid ligation buffer (Promega), linearized vector, and T4 ligase reacted at room temperature for 30 min before bacterial transformation. Homemade DH5α *E. coli* competent cells were used for all bacterial cloning experiments. Miniprep (QIAprep Spin Miniprep Kit, Qiagen, USA) was used to purify plasmids according to modified manufacturer's protocol. The linearized vector (100–400 ng) was used as a template for *in vitro* RNA transcription using the MEGAshortscript T7 kit (Ambion/Invitrogen) following the manufacturer's instructions.

2.3. Generating mutant lines

Each single-cell embryo was microinjected with approximately a 500-picoliter mixture solution containing 100 ng/μl of sgRNA and 150 ng/μl of Cas9 mRNA. Approximate 400 single-cell embryos were microinjected within 30 min of successful spawning. Microinjection was driven by compressed N2 gas under control of PV820 Pneumatic PicoPump (World Precision Instruments, Sarasota, FL), accomplished using a microcapillary pipette attached to a micromanipulator, under a Leica MZ6 microscope (Leica, Germany).

Thirty embryos (F0) per microinjected cohort were collected for estimating gRNA efficiency at 48 hrs post fertilization (hpf). Genomic DNA was extracted by incubating embryos in 50 mM NaOH at 99 °C for 20 min. The supernatant (containing DNA) was obtained by centrifugation and used directly in PCR. PCR primers were designed around the gRNA target and used to amplify the target region. PCR conditions: Initial denaturation for 2 min at 94 °C; 35 cycles of denaturation at 94 °C for 30 s, annealing at 57 °C for 30 s, elongation at 68 °C for 30 s, then a final step at 68 °C for 10 min.

If pooled F0 embryos had undigested bands after treatment with the restriction enzyme VSP1 (AseI, Thermofisher, #ER0911), then Cas9 successfully cut the targeted region and the cell repaired damage, destroying the restriction enzyme site and possibly creating a frameshift mutation. The remaining embryos of the clutch were raised to adulthood and out-crossed with *wt*. F1 embryos were screened as previously described at 48 hpf, and mutations were confirmed by DNA sequence at the in-house genomic DNA sequencing facility. Heterozygous F1 embryos with frame-shift mutations were grown to adulthood and individuals were screened by fin clipping and RE digestion. Individuals that were heterozygous for the same mutation were paired for spawning. F2 and embryos from subsequent generations were collected and grown into adulthood where they were screened as described previously. Specific mutation was also confirmed in the transcripts using cDNAs from brain or ovarian samples and PCR primers in different exons (Table 1). Subsequent generations were crossed with matching genotypes, grown into adults, and screened as previously described.

2.4. Gonadal sex determination and histology analyses

All the fish used for gonadal sex determination were between 3- and 7-month old mature adult fish. Gonadal sex was assessed initially by dimorphic body shape and color of zebrafish. A male zebrafish typically has a flat and slender belly and appear to be more gold or yellow in body color. A female zebrafish has a round belly and light body color. Then, the gonadal sex of each fish was evaluated based on typical morphology of ovary or testis under a stereo microscope, finally determined based on presence of oocytes or sperms followed by histology

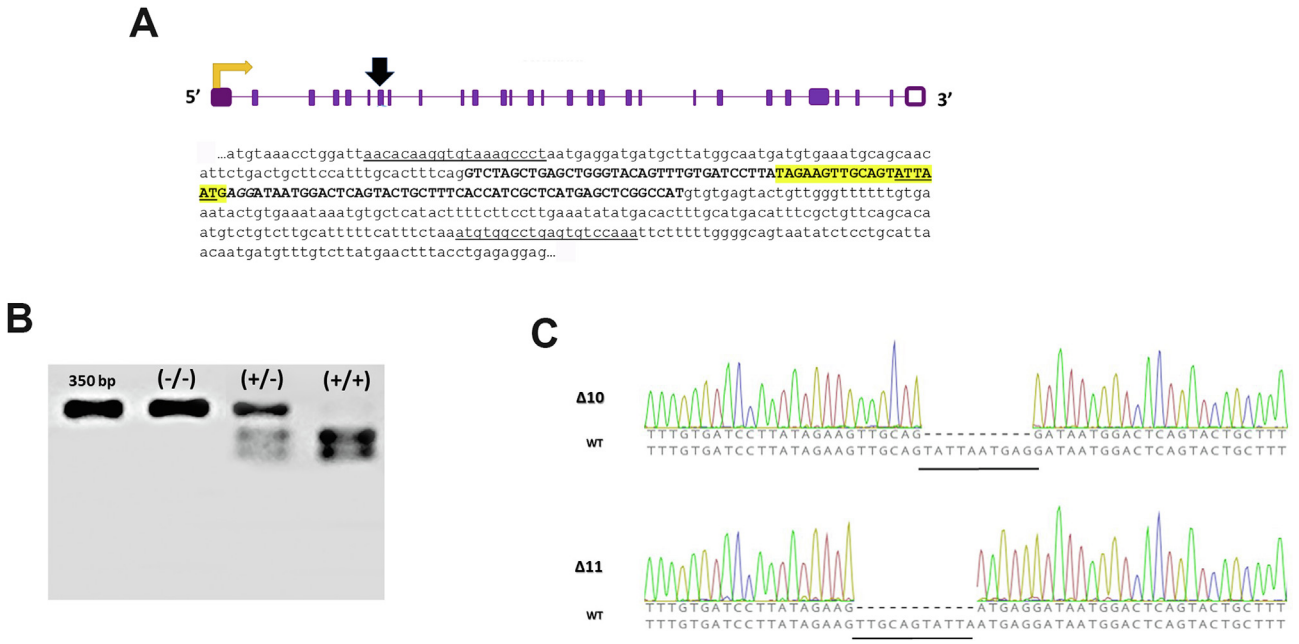

Fig. 1. Targeted and heritable genetic modification of *adamts9* (gene) in zebrafish. (A) Schematic drawing shows organization of introns and exons of *adamts9* and location of CRISPR/Cas9 targets indicated by a downward arrow. The gRNA targeting exon 7 was successful in inducing mutations. Nucleotide sequence of exon 7 and its flanking regions of *adamts9* is displayed. Lowercase: intron. Capital: 7th exon. Underlined: PCR primer pairs. Highlighted: gRNA targeted sequence. Highlighted and underline: Ase1/Vsp1 restriction enzyme site. Italics only: PAM site. (B) Restriction enzyme analysis of PCR products amplified from genomic DNA of tail fin of wildtype or *adamts9* mutants. PCR products were subjected to AseI restriction enzyme digestion. Homozygous (−/−) samples lost the recognition site and were not digested. Heterozygous (+/−) samples had both a mutated and *wt* (+/+) allele, resulting in 3 distinct bands when ran on an agarose gel. (C) Sequence of *adamts9* genomic DNA identified two mutant lines. One mutant line had 10 nucleotide deletions (Δ 10; TATTAATGAG), while another mutant line had eleven (Δ 11; TTGCAGTATTA). Underlined is deleted nucleotide sequence compared to *wt* sequence.

analyses.

Fish were sacrificed in the late afternoon unless indicated otherwise using ice water in accordance to IACUC guidelines. Once heart function ceased, they were humanely decapitated by serving spin cord and placed in 10% buffered formalin (Fisher Scientific) for 24–48 h before the gonad was dissected. The gonad was then placed in formalin for an additional 24 h. After gonads were fixed, they were prepared for histological analyses with either paraffin or JB4. These mounting mediums share the dehydration process but use different procedures for infiltration.

Infiltration/embedding with paraffin: Samples were placed in xylene (StatLab) for 30 min on the tissue rocker, then an additional 30 min in an incubator (55–60 °C). Paraffin (Fisher Scientific, T565) was added in a 1:1 ratio with xylene, placed in the incubator, and gently shaken every 10 min for 30 min. The sample tissue was then transferred to fresh, 100% paraffin, and shaken every 15 min for 1 h in the incubator (paraffin was changed after 30 min). Then was placed in a block mold, covered with fresh paraffin, and allowed to cool overnight.

For JB-4 infiltration/embedding: JB-4 solution A was made according to manufacturer's instructions (00226, Polysciences Inc., PA). The dehydrated gonads were placed in 1 mL of JB-4 solution A on the tissue rocker for 1 h, with solution changed after 30 min. After an hour in JB-4 solution A, samples were removed from solution and oriented in JB-4 block holders (15899-50, Polysciences Inc., PA). The embedding solution was freshly made, cold JB-4 solution A and room temp JB-4 solution B. They were mixed briefly then immediately transferred into the block using a disposable pipette. Blocks were held on a Styrofoam conical tube holder, and samples polymerized for 72 h before sectioning.

Paraffin and JB4 embedded samples were cut into 10 μM and 5 μM sections, respectively using a microtome (Reichert-Jung, 2030) and coated metal blades (95057-834, VWR). Hematoxylin and eosin (H&E) staining was done immediately following the last step of deparaffinization. Slides were kept in xylene until cover glass (12-541-B, Fisher Scientific), was mounted using Permount (SP15-100, Fisher Scientific).

2.5. Immunocytochemistry

After the formalin-fixed paraffin embedded samples were sectioned, glass slides of *adamts9*$^{-/-}$ and *wt* were used for immunohistochemistry staining using Vectastain Elite ABC kit (PK-6101, Vector Laboratories, CA). Antigen retrieval was conducted by incubating slide sections with 0.1% testicular hyaluronidase (H3506, Sigma, USA) in 30 mM NaOAc and 125 mM NaCl (pH 5.2) for 2 h at 37 °C. Slides were rinsed with distilled water for 5 min before being washed with 1× PBS three times, for 3 min each. To quench endogenous peroxidase activity, slides were treated with hydrogen peroxide solution for 30 min and were washed with 1× PBS as described previously. Normal goat serum was made according to manufacturer's instructions and incubated for 30 min to

Table 1
PCR primer sequences and conditions for amplification of *adamts9* cDNAs. Primers were designed so PCR product would span multiple exons to reduce the chance of amplifying genomic DNA.

cDNA Primer	Forward Sequence	Reverse Sequence	PCR Product Length (bp)	Annealing Temp (°C)	Extension Time (s)
ADAMTS9-7	AATGAGCTGGATGGACCCAC	CACCATACCCTGTGTCGAGG	442	61.4	45
ADAMTS9-8	AGGTCTAGCTGAGCTGGGTA	ACCGGCTCATCAAGCAAACA	291	57	30

block non-specific binding sites before applying the primary antibody. Sections were incubated with primary antibodies (Triple point biologics, Inc., OR) RP1 (250× dilution, RP1-ADAMTS-9) and RP5 (1000× dilution, RP5-ADAMTS-9) overnight at 4 °C. As a negative control, additional sections were also incubated under same condition except using unvaccinated normal rabbit serum. The next day slides were washed with 1× PBS as described earlier. The secondary antibody was made according to manufacturer's instructions and incubated with slides for 30 min. While slides were incubating with the secondary antibody, the AB solution was made according to manufacturer instructions. Slides were washed with water and 1× PBS again before applying AB solution and incubated for 30 min. Another wash with 1× PBS was done before developing slides in 50 mM Tris (pH 7.2) containing 100 mg DAB (3,3′-Diaminobenzidine. D12384, Sigma) and 75 µL of 30% H_2O_2, for exactly 2 min. Adjacent sections were stained with H&E for structural comparison.

2.6. Spawning and fertility

To determine spawning rate and fertility, a male and a female were paired in a labeled polycarbonate breeding tank on the work-bench, separate from the automatic rearing system. Every afternoon they were fed as previously described. An hour before the lights turn off, their water was changed, and an insert was placed inside of the tank to allow eggs through to the bottom, preventing adults from eating them. The morning of next day (11 AM), the water was changed. The collected eggs were placed in an incubator (28.5 °C) and grown for an average of 10 days before being put on the automatic system (fry were fed ground commercial food starting 3dpf, freshly hatched artemia 7dpf). If paired fish didn't spawn after one week, they were placed with another partner that has spawned previously. The partner was replaced with another individual of the same sex, before repeating the process with the opposite sex. Fish were considered infertile when no spawning was observed after being paired with six partners (3 males and 3 females).

2.7. Survival assay

To determine the survival rate of fry, adult fish were observed spawning regularly for two weeks before their fry were collected for study. At least 5 pairs (5–31 pairs) and multiple clutches from each adult pair were used for the experiment. Eggs collected from each parent were counted, labeled, and separated into breeding tanks containing an average of 40 eggs per tank. Survival after 24 h, 7 days, and 14 days was found by tracking the number of dead fish found during the daily feeding and water change. The survival rate was calculated by taking the percentage of surviving fish from the initial egg count.

2.8. Statistical analyses

Students' *t* test (unpaired) was used to determine significant differences between two data sets (expected vs experimental percentages of genotypes) and one-way ANOVA followed by Tukey's test was used for comparing more than three data sets (GSI%) with GraphPad prism software (GraphPad Software, Inc., San Diego, CA.

3. Results

3.1. Generating mutant lines

The zebrafish Adamts9 protein is composed of 1643aa with a signal peptide, prodomain, metalloproteinase domain, cysteine rich domain, and multiple thrombospondin repeats (Fig. 2A). Two mutant zebrafish lines (Δ10 and Δ 11) that had deletions which generated premature stop codons before the enzymatic active site (at 573aa) were selected and propagated (Figs. 1 and 2A). Genomic mutations were found to be conserved in the cDNA sequence of homozygous samples (Fig. 3).

To determine whether Adamts9 protein is present in the knockout, two commercial antibodies were used in immunohistochemistry (IHC); the RP1 antibody against the human ADAMTS9 pro-domain (human sequence is a 41% match to zebrafish), and the RP5 antibody against human ADAMTS9 catalytic domain (human sequence is an 85.7% match to zebrafish). IHC using the RP1 antibody revealed that Adamts9 was expressed specifically in the follicular cells of *wt* (Fig. 2C and c). In *adamts9*$^{-/-}$, follicles of similar size and structure to *wt* (Fig. 2b′) had no detectable signal from the follicular cells (Fig. 2c′). IHC with the RP5 antibody also found that Adamts9 was expressed specifically in the follicular cells of *wt* zebrafish with a distinct, discontinuous pattern (Fig. 2D and d). The same antibody stain on *adamts9*$^{-/-}$ follicles of a similar size revealed that the structures were similar, but there was no detectable signal from the follicular cells (Fig. 2d′). This result suggests truncated protein was not produced or dumped by the cells. Therefore, the generated *adamts9*$^{-/-}$ zebrafish mutant lines will be referred to as knockouts due to the lack of detectable Adamts9 protein.

3.2. Low survival of homozygous progeny

F2 and subsequent generations of heterozygous fish were in-crossed and screened to determine their genotypic ratio. The overall percentage of *adamts9*$^{-/-}$ knockouts that were found was 11% at 1-month post fertilization (mpf) and 4% at 3 mpf (Table 2), significantly less than what was expected from *adamts9*$^{+/-}$ Mendelian crosses (25%). To investigate the low number of *adamts9*$^{-/-}$ knockouts found, we asked whether there was a difference in number of eggs released or the initial survival of fry from *adamts9*$^{+/-}$ and *wt* pairs. The number of eggs released and their survival were monitored daily for a week, and no difference was found between *wt* or *adamts9*$^{+/-}$ clutches for the average number of eggs released/day (Fig. 4A), or the survival of those eggs for the first week (Table 3). But, at 14dpf there was a significant decrease in the survival of the heterozygous progeny (Table 3).

3.3. Male biased sex ratios and female infertility in adamts9$^{-/-}$

Adamts9$^{+/-}$ and *wt* fish were found to have similar male to female ratios within the same tank (about 2:1), but the homozygous fish were overwhelmingly male (37/45; 82%) when fish were 3–7 months old (Fig. 4B). Most homozygous mutant males (28/36; 77%) were able to fertilize *wt* eggs (data not shown). Only a few homozygous females (3/45; 7%) were found, and none of them were able to spawn. Strikingly, a significant number of individuals had empty, a pair of ovarian-like membranous shells (5/45; 11%, Fig. 5C3), but their gonadal shells were observed to produce mature sperm on the periphery of these transparent shells upon histological analysis (Figs. 5C4, 6). However, these individuals were infertile, and no viable embryos were observed when paired with *wt* females or male spawning partners.

3.4. No obvious reproductive defects in adamts9$^{-/-}$ males

Most adult (7 mpf) *adamts9*$^{-/-}$ males had similar fertility (data not shown) and body shape to those of their *wt* counterparts' despite spinal deformity (Fig. 5, columns A and B). The *adamts9*$^{-/-}$ testes had similar morphology as those of *wt* (Fig. 5, A3 and B3). In the *wt* sample, testis had very distinct spermatogenic cysts (Fig. 5, A3), whereas the homozygous cysts were less defined (Fig. 5, B3). Closer examination is needed to determine if less-defined cysts are a phenotype of the knockout or an individual trait.

Histological analyses of the testis further revealed that the relative size and amount of spermatogonia were similar to the density of mature spermatozoa (Fig. 5, A4 and B4). There was extra space between spermatogenic cysts within the *adamts9*$^{-/-}$ testis, but this might be an artifact of the fixation process. No obvious differences between *wt* (Fig. 5, A4) and *adamts9*$^{-/-}$ (Fig. 5, B4) males were observed.

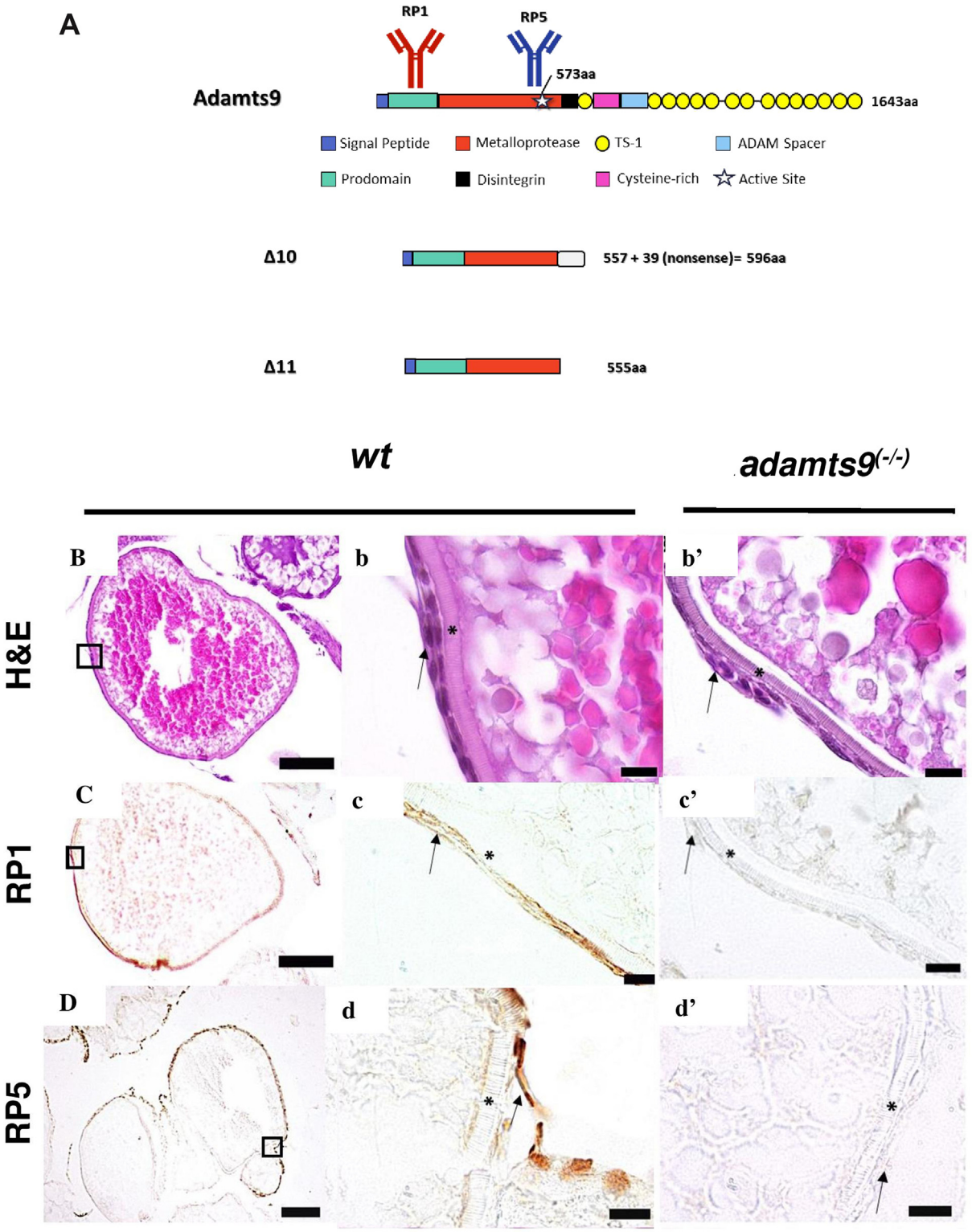

Fig. 2. Confirming adamts9 knockout by immunohistochemistry. (TOP: A) Schematic drawing of various functional domains of zebrafish Adamts9 protein and predicated truncated proteins for each mutant line. The Δ 10 mutation started nonsense sequence at aa 557 and stopped at 596aa, whereas Δ 11 mutation had a premature stop at aa 555. In both cases the mutation lost the active site of Adamts9 (aa 573). Corresponding positions of two commercial antibodies against the prodomain (RP1) and metalloprotease (RP5) domains of human ADAMTS9 are shown. Hematoxylin and Eosin (H&E) (Row B) and immunohistochemistry staining (Rows C-D) of stage IV fully-grown immature follicles from wildtype (*wt*) or *adamts9* mutant zebrafish using primary antibodies against the prodomain of human ADAMTS RP1 (C) (Triple Point Biologics, catalog# RP1-ADAMTS9, has 41% sequence identity to zebrafish Adamts9) or RP5 (D) (Triple Point Biologics, catalog# RP5-ADAMTS-9, has 81% sequence identity to zebrafish Adamts9). As a negative control, additional sections were also stained with primary antibodies omitted (data not shown). H&E sections were adjacent to those used for immunohistochemistry to show the structure of the oocyte (B-b′). Low (uppercase letters) magnification images of a representative stage IV follicle. Boxed areas are 40× enlarged (lowercase letters). High magnification (40×) representative immunostaining of stage IV follicles from *adamts9*$^{-/-}$ with the antibody against human ADAMTS9 RP1 (c′) and RP5 (d′). Zona pellucida is indicated by *, Arrow points to follicular cells.

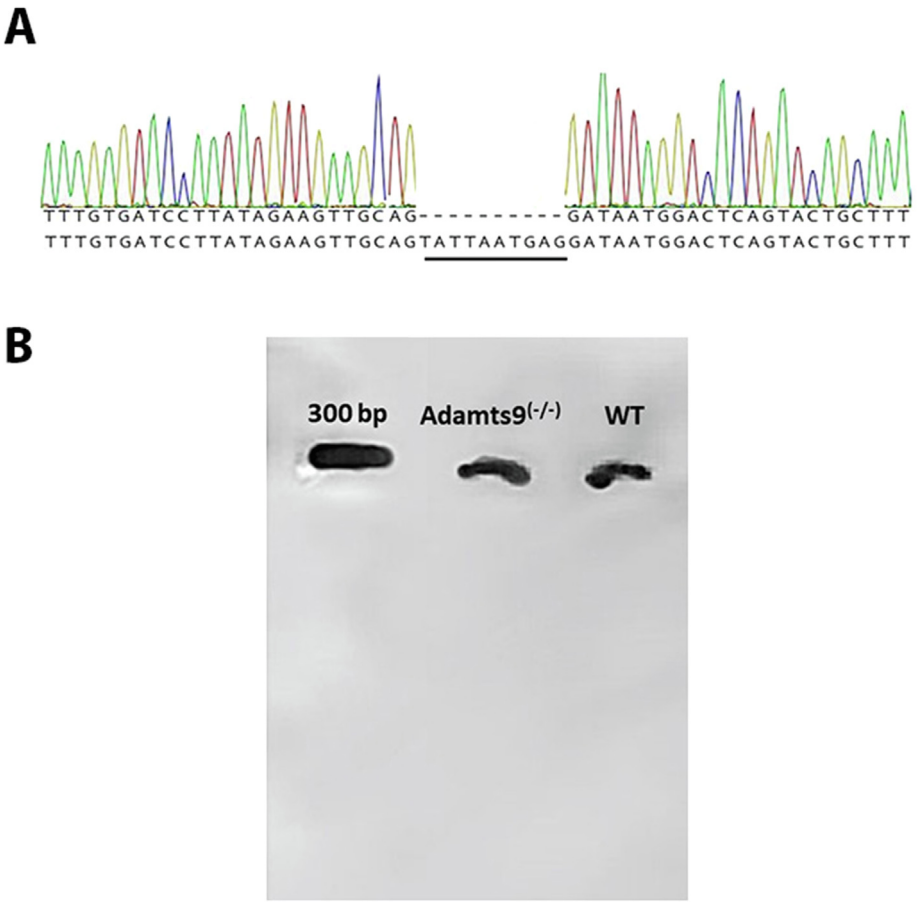

Fig. 3. Mutations confirmed in *adamts9* mRNA. (A) Comparison of *adamts9*$^{-/-}$ cDNA sequence to *wt*. Underlined is deleted nucleotide sequence compared to the *wt* sequence. (B) Representative PCR products amplified from cDNAs of wildtype (*wt*) or *adamts*9$^{-/-}$.

Table 2
Genotype ratios from *adamts9* heterozygous in crossings. Expected a Mendellian ratio of 25% *wt*, 50% (+/−) and 25% (−/−). At 1 mpf (month post fertilization) only 11% of 90 fish screened were homozygous mutants, which was reduced to only 4% when older than 3 mpf.

Genotype	Expected value (Mendelian Ratios)	Experimental value: 1 mpf	Experimental value: > 3 mpf
wt (*adamts9*$^{(+/+)}$)	25%	38.9%	40.2%
adamts9$^{(+/-)}$	50%	50.9%	55.7%
adamts9$^{(-/-)}$	25%	***11.1%****	***4.1%****
	N =	90	1047

*: indicate significant difference between expected Mendelian value (25%) and experimental value ($p < 0.001$).

3.5. *Adamts9*$^{-/-}$ *females has malformed ovaries*

Overall, adult (7mpf) *adamts9*$^{-/-}$ females resemble the body shape of their *wt* counterparts despite spinal deformity (Fig. 5, columns D and E). The *adamts9*$^{-/-}$ female ovary (Fig. 5, D2) covered less surface area than *wt* (Fig. 5, E2) when comparing their open abdomens. Mutant females had less of large ova and more interstitial space (Fig. 5, D3). Dissected *wt* ovaries showed hundreds of visible eggs and very little interstitial tissue (Fig. 5, E3). Histological analyses of homozygous ovaries found they had fewer vitellogenic oocytes (some degenerating), relatively high amounts of early stage I oocytes, and the ovaries themselves were smaller overall (Fig. 5, D4). *Wt* ovaries showed that hundreds of eggs concurrently develop, with the most eggs in an intermediate stage (II–III), and less in (early) stage I or (late) stage IV (Fig. 5, E4).

3.6. *Female-like Adamts9*$^{-/-}$ *male gonads lack majority of internal structure*

Female-like *adamts9*$^{-/-}$ male fish (Fig. 5, column C) outwardly resemble *wt* female fish in color and body shape, retaining slight spinal malformations characteristic of *adamts9*$^{-/-}$ mutants (Fig. 5, C1). Remarkably, upon removal of the abdominal wall the body cavity appears to be empty, except for organs that normally surround the gonad (like the intestines, stomach and swim bladder), which were morphologically *wt* despite excess space (Fig. 5, C2). Surprisingly, when the mutant was submerged in water to take higher resolution pictures, an ovarian-like, membranous structure inflated and was observed in the empty space (Figs. 5, C3; 6, A). Upon histological analyses, there was a surprising absence of tissue and cells within the membrane when comparing this structure to ovaries of *adamts9*$^{-/-}$ or *wt* (Fig. 5, C4). On the periphery of the membranous, ovarian-like structure in most *adamts9*$^{-/-}$ samples were spermatogenic cysts that contained mature sperm (Figs. 5, C4; 6, A1-2). Intriguingly, one critical female-like sample had both early-stage ova and testis-like cysts (Fig. 7).

3.7. *Adamts9*$^{-/-}$ *have multiple uncharacterized phenotypes*

When screening adult fish (3–7 mpf), homozygous mutants were visibly smaller than their *wt* counterparts (data not shown). After screening, knockouts were grown in low-density tank conditions (> 10 fish/tank) for an average of two weeks to be large enough for spawning experiments (data not shown). Most adult *adamts9*$^{-/-}$ (41/47) had visible spinal deformities in the midbody and/or caudal peduncle

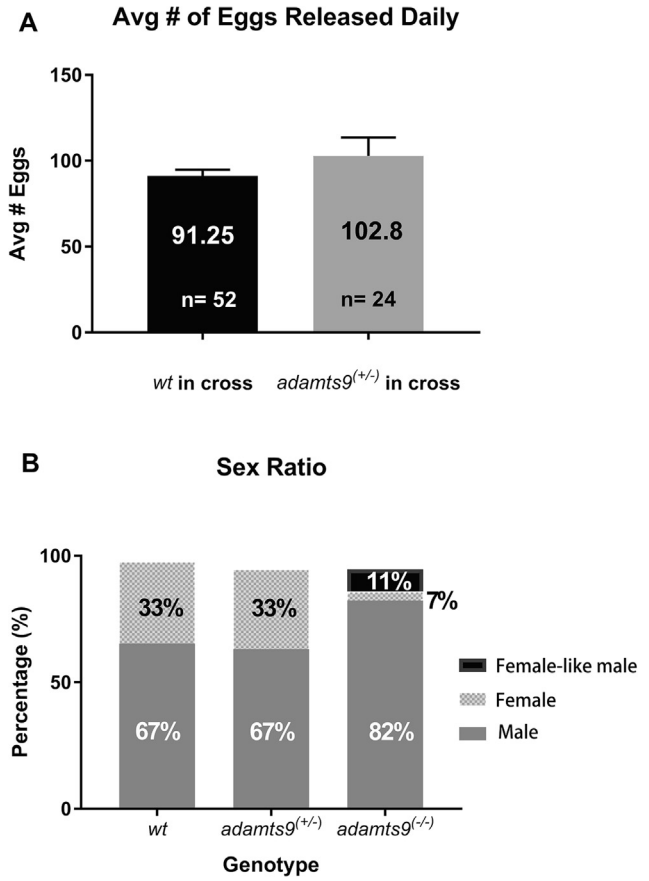

Fig. 4. Male biased sex ratios and female infertility in *adamts9*$^{-/-}$ (A) Daily embryos produced averaged from numbers of embryos collected over 2 weeks from wildtype (*wt*) or *adamts9*$^{+/-}$ in-cross. Adamts9$^{+/-}$ fish were paired together to generate homozygous fish. After spawning regularly for a week, embryos were collected and counted for two weeks. Number of pairs are represented by n, an average of 4 samples were collected from each pair. (B) Sex ratios among offspring from *adamts9*$^{+/-}$ in-cross. *wt* and *adamts9*$^{+/-}$ fish had a 2:1 ratio of male to females in fish older than 3 mpf. Most homozygous fish were male (82%) and fertile, only 3 females (7%) were found but they were not able to spawn. There was also a group of female-like male fish found that did not have normal gonad morphology and instead had empty membrane bound compartment (11%). *wt* total n = 118, male = 79 (67%), female = 39 (33%); *adamts9*$^{+/-}$ total n = 192, male = 128 (67%), female = 64 (33%); *adamts9*$^{-/-}$ total n = 45, male = 37 (82%), female = 3 (7%), female-like male = 5 (11%).

Table 3
Survival rate following fertilization (24 h, 7 days, and 14 days). At 14 days wildtype (*wt*) fish had slightly reduced survival rate, but (+/−) in cross had significantly more death at this time. 24 hpf (hours post fertilization): *wt*, 31 pairs, 81 clutches; (+/−), 18 pairs, 25 clutches. 7 dpf (days post fertilization): *wt*, 15 pairs, 37 clutches; (+/−), 10 pairs; 16 clutches. 14 dpf: *wt*, 5pairs, 4 clutches; (+/−) 5 pairs, 6 clutches.

Age	Percent survival of *wt* in cross	Percent survival of adamts9$^{(+/-)}$ in cross
24 hpf	94.2%	89.9%
7 dpf	93.4%	94.26%
14 dpf	77.9%	***51.33%****

*: indicate significant difference between WT survival and heterozygous incross ($p < 0.05$).

(Fig. 5, B–D) in a left/right direction. There were *wt* fish that also had spinal deformities, but their malformations were dorsal/ventral (data not shown). The identity of affected vertebrae, when the malformation is first visible, or differentially expressed morphogenic factors have not been determined.

4. Discussion

4.1. Heterozygous crossings yield low percentage of homozygous progeny

Indicative of congenital disease and early death, *adamts9*$^{-/-}$ zebrafish are found in ratios well below that predicted by Mendelian genetics. Many *adamts9*$^{-/-}$ zebrafish have lateral spinal deformities in the midbody or caudal peduncle and grow slower compared to *wt* fish. Zebrafish are known to continuously grow until around 6 months post fertilization (Singleman and Holtzman, 2014). Growth retardation and spinal curvature often indicate congenital cardiac and renal abnormalities in humans (Janicki and Alman, 2007). Adamts9 is known to be lost in hereditary renal tumors (Clark et al., 2000) and *adamts9*$^{+/-}$ mice have valvular and aortic abnormalities (Kern et al., 2010). Homozygous *adamts9*$^{-/-}$ mutations are embryonically lethal in mice, which hampers our understanding of *adamts9* functions in adult vertebrates (Jungers et al., 2005). Our study provides the first global knockout vertebrate model that will permit investigation of *adamts9* functions in the development and in adult vertebrates.

For embryos to develop correctly, proteoglycans in ECM must be correctly glycosylated for metalloproteases to release bioactive domains. If insulin receptivity is reduced during embryonic development, cells cannot recognize or uptake glucose, resulting with the disruption of glycosylation and arrested growth (Benz et al., 2016). Numerous gene association studies have implicated that a gene variant of ADAMTS9 (rs4607103) is associated with insulin resistance and beta cell function in human type II diabetes (Meigs et al., 2008; Tam et al., 2013). Further evidence supporting the role of adamts9 and insulin receptivity comes from a genetic study of *C. elegans*. Researchers found that GON-1, an *adamts9* ortholog, is required for normal insulin signaling in beta cells and peripheral tissue (Yoshina and Mitani, 2015), and insulin-like signaling in mutant phenotypes was partially rescued by overexpression of the c-terminal GON domain (Yoshina and Mitani, 2015). The GON domain is incorporated in multiple secreted proteins that may indirectly or directly impact insulin signaling of many species (Benz et al., 2016). There are 19 metalloproteases in the vertebrate *adamts* family, but only *adamts9* and *adamts20* retain the c-terminal GON domain. (Somerville et al., 2003). Yet, the NIH gene database suggests that the GON domain is absent in zebrafish *adamts9* (Brunet et al., 2015). Regardless if zebrafish are naturally missing the GON domain or not, functional compensation by related metalloproteases like *adamts20*, may explain why *adamts9*$^{-/-}$ zebrafish survive gastrulation. Insufficient insulin signaling, renal, and cardiac abnormalities could be responsible for the increased death rate in juvenile *adamts9*$^{+/-}$ clutches (Table 2).

4.2. Most adamts9 (−/−) fish are male

Zebrafish are a gonochoristic species (two distinct sexes) of teleost that utilize transitory hermaphroditism, where all juveniles first form undifferentiated ovaries containing primordial oocytes before undergoing apoptosis to develop as testes (Takahashi, 1977). In the early testis, primordial oocytes undergo a highly dynamic, poorly understood process which leaves cavities that fill with clusters of cells reported to be testicular germ cells (Orban et al., 2009). Unlike mammals, zebrafish lab strains lost their chromosomally determined sex locus and instead rely on multiple factors, including the amount of germline precursor cells, to support gonadal development (Liew and Orbán, 2014).

In zebrafish, the number of primordial germ cells (PGCs) are critical for the formation of ovaries (Siegfried and Nüsslein-Volhard, 2008). Ablation or loss of PGCs entirely during development produce sterile males with no proliferating germ cells (Tzung et al., 2015), but reducing the number of PGCs while the fish are juveniles or adults allows

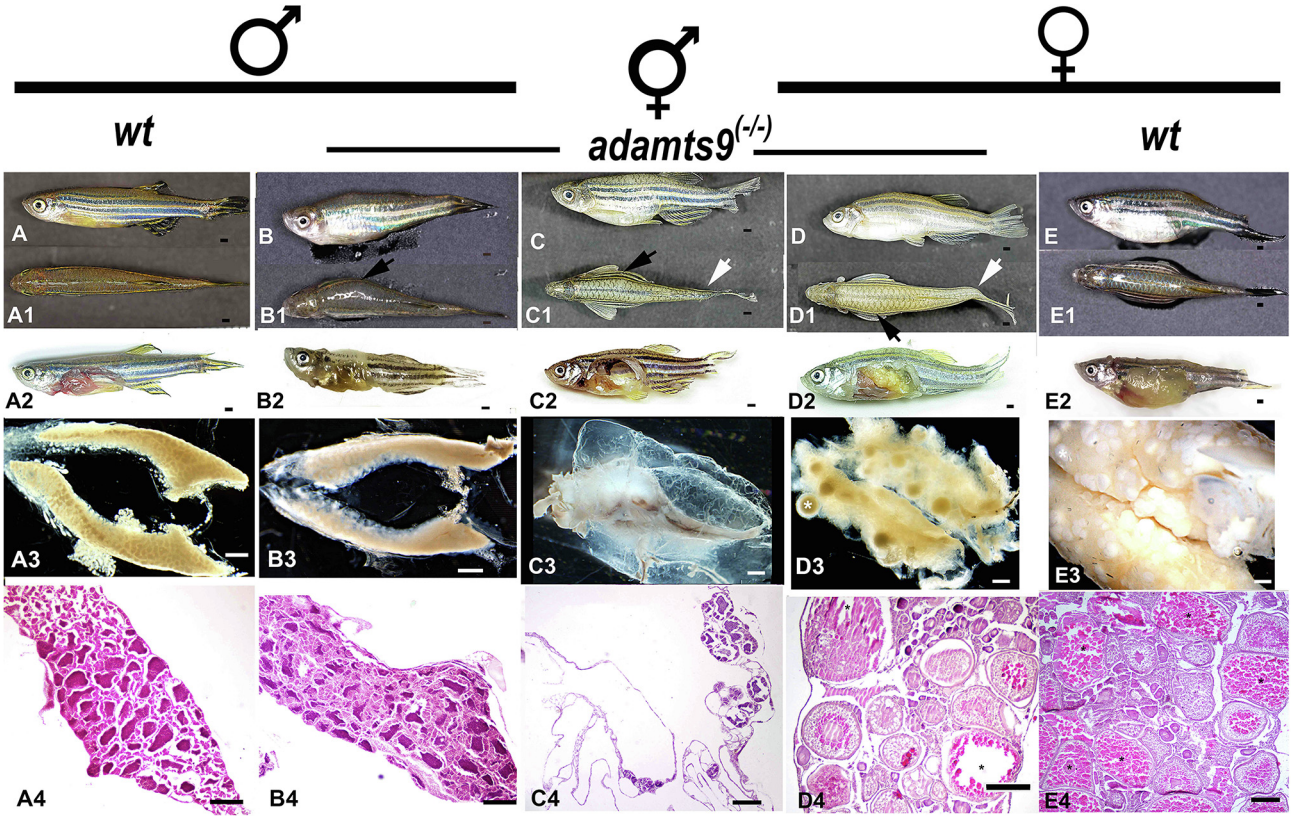

Fig. 5. Comparison of external appearance and gonadal morphology of wildtype (*wt*) and *adamts9*$^{-/-}$ fish. Top row (A–E. Scale bar is 1 mm) are side view of representative fish of *wt* male (A), *adamts9*$^{-/-}$ male (B), female-like *adamts9*$^{-/-}$ male (C), *adamts9*$^{-/-}$ female (D), and *wt* female (E). Row 1 (A1–E1. Scale bar is 1 mm) is top view of *wt* male (A1), *adamts9*$^{-/-}$ male (B1), female-like *adamts9*$^{-/-}$ male (C1), *adamts9*$^{-/-}$ female (D1), and *wt* female (E1). Arrows indicate spinal malformity in mid-body (black) and caudal peduncle (white). Row 2 (A2–E2. Scale bar is 1 mm) is comparison of open abdominal cavity. Testis are difficult to see between swim bladder and intestine in *wt* (A2) and *adamts9*$^{-/-}$ (B2) male fish. Ovaries take up most of the space in *wt* female (E2), but *adamts9*$^{-/-}$ females had longer, thinner ovaries (D2). Strikingly, female-like *adamts9*$^{-/-}$ male fish appeared empty (C2). Row 3 (A3–E3. Scale bar is 1 mm) is comparison of entire gonad. Testis of *wt* (A3) and *adamts9*$^{-/-}$ (B3) male fish were similar. Ovaries of *wt* female (E3) were opaque with thousands of eggs within the organ. *Adamts9*$^{-/-}$ females had smaller ovaries with fewer visible eggs and excess undifferentiated tissue (D3). Female-like *adamts9*$^{-/-}$ male fish had membranous sac lacking internal structure and was taken at lower magnification (C3). Large eggs = (White)*. Row 4 (A4–E4. Scale bar is 200 μm) is hematoxylin and eosin (H&E) staining of gonadal sections. The gonad from Female-like *adamts9*$^{-/-}$ male fish lacked internal cellular structure with spermatogenic cysts along the periphery (C4). Stage IV oocytes (*) were visible in both *wt* or *adamts9*$^{-/-}$ female ovaries but homozygous females (D4) had fewer stage IV eggs, a greater amount of stage I–II oocytes, and more interstitial space.

them to differentiate into fertile males (Dranow et al., 2013; von Hofsten and Olsson, 2005; Webster et al., 2017). *Adamts9*$^{-/-}$ clutches are overwhelmingly male, similar to the phenotype that arises from reduced numbers of PGCs in juveniles. It is possible that the PGCs in *adamts9*$^{-/-}$ mutants do not migrate or proliferate properly, like GON-1 knockouts in *C. elegans* (Blelloch and Kimble, 1999) and Adam-TS knockouts in *Drosophila* (Ismat et al., 2013). Migration problems arising from *adamts9*$^{-/-}$ zebrafish could also give rise to male-biased populations in adult zebrafish. Although, the mismigration or inability of PGCs to proliferate would not fully explain the several females and the female-like male mutant fish that were found. The presence of retained oocytes along with the loss of tissue in fish implies *adamts9* may play a role in the regeneration somatic tissue surrounding oocytes.

Plasticity in teleost fish is well documented (Santos et al., 2017), but the plasticity of the mammalian gonad is less understood (Deliagina et al., 2002). There are only two documented cases of mammalian gonads exhibiting plasticity after birth in XX (female) knockout mice: FoxL2 and ESR1/2 (Couse et al., 1999; Uhlenhaut et al., 2009). As young adults (3–4 weeks), female knockout mice had functional ovaries but between 8 weeks and 3 months ovarian follicular cells (granulosa and theca) reorganized, and the gonadal RNA expression profiles as well as morphology resembled testis-like support cells (Sertoli and Leydig) (Couse et al., 1999; Uhlenhaut et al., 2009). Teleost fish and mammals differ on the upstream (master) switch for sex determination, but many key transcription factors that drive sexual differentiation- like SOX9 and FOXL2, are conserved (Siegfried and Nüsslein-Volhard, 2008; Sun et al., 2013). Genes activated by the FOXL2 transcription factor and estrogenic signaling may include metalloproteases that alter the extracellular matrix in the ovary, providing a viable environment for oocyte development and release.

The expression of *adamts9* in the developing and adult gonad suggests that this protein has a critical function in ovulation and sexual development. Currently, it is unclear whether the role of *adamts9* during development is similar in adult tissue, or if there are distinct functions during each period. Although *adamts9*$^{-/-}$ zebrafish have not been observed to ovulate, they will be indispensable to determine the signaling pathways that *adamts9* utilizes in embryonic and adult tissue.

5. Summary/conclusions

The extracellular niche is an amalgamation of multiple proteins and small signaling molecules that are needed to grow and differentiate cell-types within tissue (Brown and Badylak, 2014; Roushandeh et al., 2017). During development or after injury, the three-dimensional extracellular environment (i.e. niche) enables tissue regeneration by informing stem cells of their fate through molecular tension, and recognition of small bioactive molecules and growth factors, (Pearson et al., 2016; Demircan et al., 2013). The niche must be established and

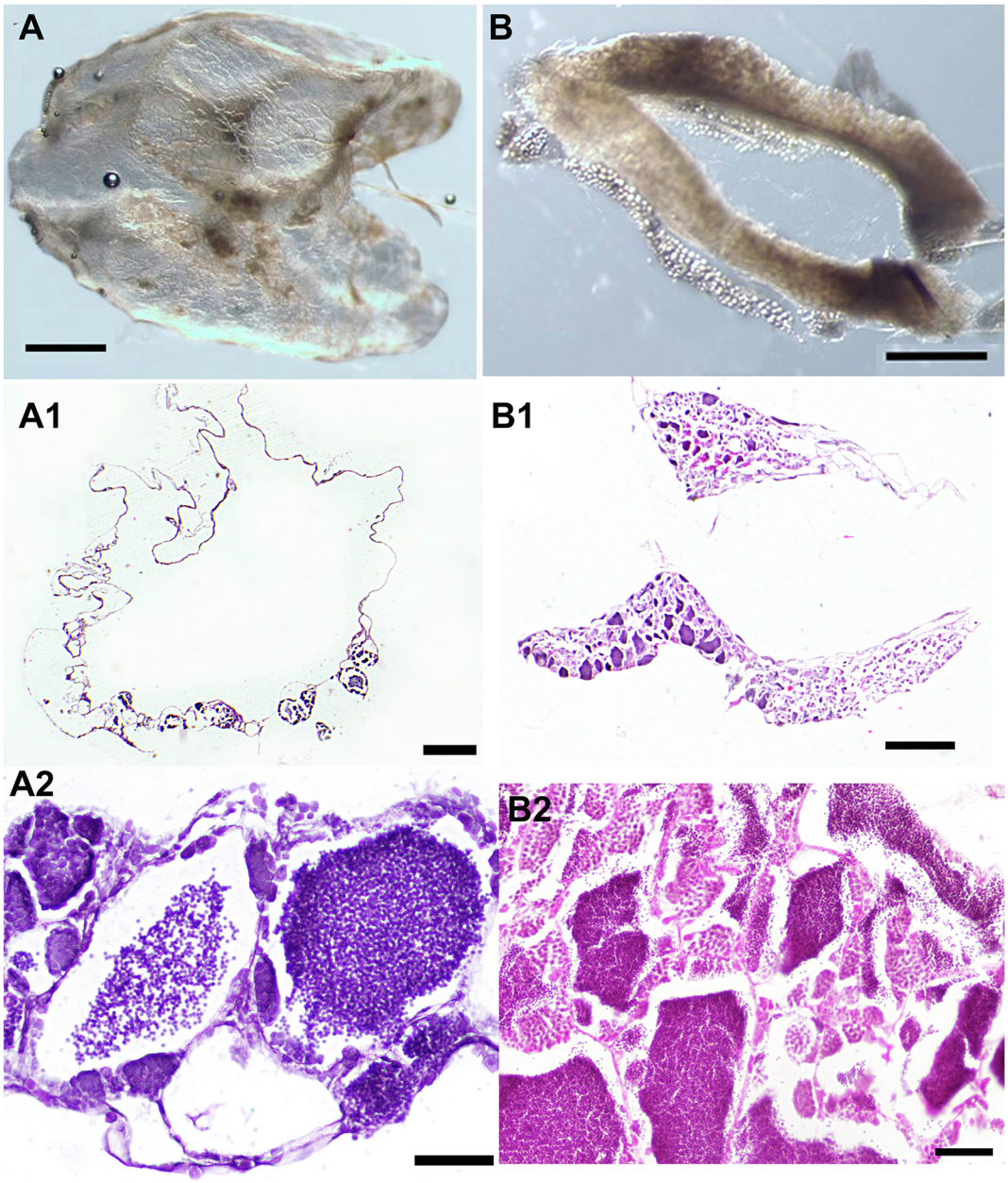

Fig. 6. Hematoxylin and eosin (H&E) stains of gonads from a representative 7-month old female-like *adamts9*$^{-/-}$ fish compared to testes from wildtype (*wt*) male. Column A: The *adamts9*$^{-/-}$ gonad is thin and transparent sac with no visible internal structures. A) Shows a pair of gonad from *adamts9*$^{-/-}$ under a stereo microscope. Scale bar is 1 mm. A1) Shows the organ was devoid of internal structure, except cysts observed along periphery area. Scale bar is 500 µm. A2) A closer look at peripheral spermatogenic cysts. Spermatogonia (sg) and spermatozoa (sz) were present. Scale bar is 50 µm. Column B: Comparison of *wt* testis, showing internal structure of organ. B) The *wt* testis were translucent and allowed light to pass through with distinct cyst structures. Scale bar is 1 mm. B1) Shows a pair of testes had multiple spermatogenic cysts throughout. Scale bar is 500 µm. B2) A closer look at *wt* spermatogenic cysts show multiple large cysts, with mature spermatozoa encircled by developing spermatocytes. Scale bar is 50 µm.

maintained to keep pluripotent cells producing daughter cells in a desired tissue (Gattazzo et al., 2014). Without the ability to regenerate granted by pluripotent progenitors, the tissue cannot heal and may become necrotic. Many organs that express *adamts9* in zebrafish are derived from the mesenchyme, including the gonadal ridges, kidney, liver, bone and heart (Brunet et al., 2015). Malfunctions of these organs during juvenile growth and development may underlie the early death observed within *adamts9*$^{(+/-)}$ (in cross) clutches (Table 3). Future investigations should focus on how these organs and related connective tissues may be afflicted in *adamts9*$^{-/-}$ knockout zebrafish.

It is known that adult female zebrafish ovaries retain germline stem cells (Wong et al., 2011). The loss of internal tissue structure in female-like *adamts9*$^{-/-}$ male fish suggests that their ovarian somatic tissue lacked regenerative capacity upon oocyte degeneration. The follicular somatic cells may turn apoptotic after a certain amount of stress, then form empty cysts because there is not a healthy supply of progenitor cells. After the degradation of a critical number of oocytes in *adamts9*$^{(-/-)}$ females, the remaining gonadal tissue could reorganize into testicular tissue- similar to experiments that ablate oocytes in adult zebrafish and give rise to male biased populations. Supporting this is a single key sample from our research captures the thin walled organ with: oocytes present, somatic cell loss and the development of sperm-like cysts, which may indicate that *adamts9*$^{-/-}$ first develop as female before the oocytes degenerate (Fig. 7). Whether these female-like *adamts9*$^{-/-}$ mutants lose gonadal structure due to inability to regenerate somatic tissue, or from some other process is a question that

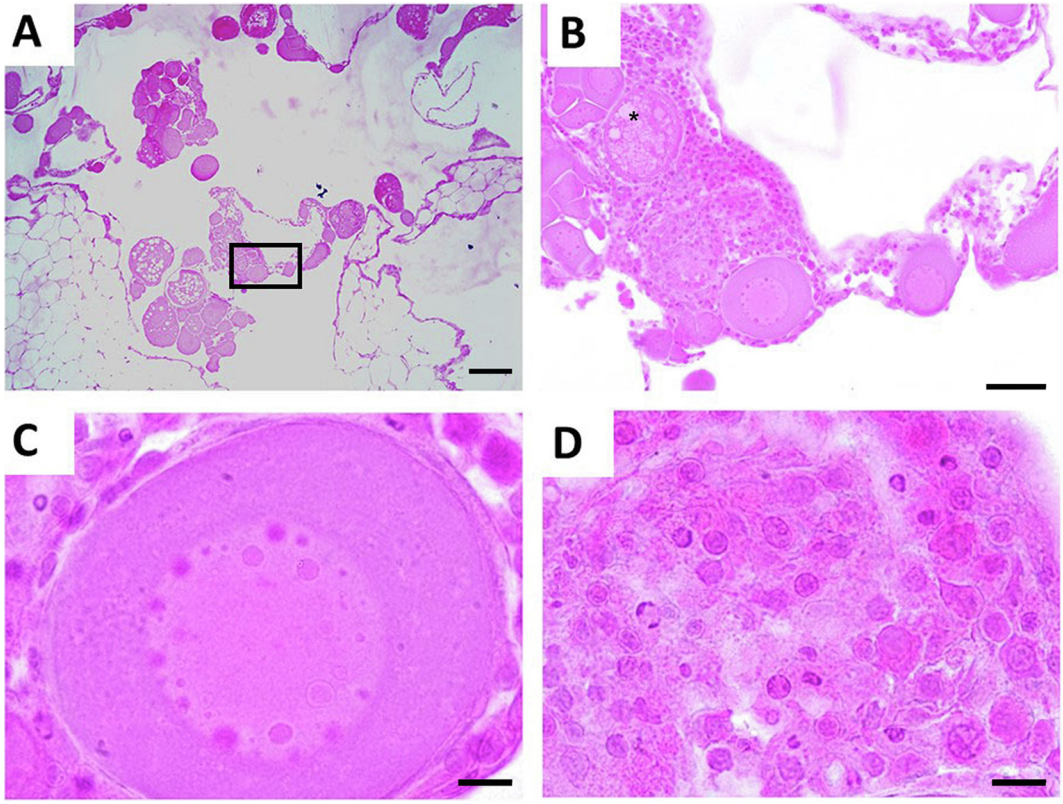

Fig. 7. Hematoxylin and eosin (H&E) stain of a representative female-like gonad containing early stage of oocytes and early spermatogenic cyst. A) A representative gonad obtained from 7-month old female-like fish with largely empty space and few oocytes along the periphery. Scale bar is 200 μm. B) Enlarged area boxed in picture A showing oocytes (one degrading = *) along with increased interstitial tissue that resembles early spermatogenic cysts. Scale bar is 100 μm. C) High magnification of oocyte and its follicular cell layer. D) High magnification of interstitial tissue resembling distinctly shaped nuclei of spermatogenic cyst. Scale bar for picture C & D is 10 μm.

has yet to be investigated.

In summary, this is the first study producing vertebrate *adamts9* knockouts that survive until adulthood, providing a model for studying the functions of *adamts9* in the development and in adult vertebrates. Our study reveals the necessity of *adamts9* for the proper development and upkeep of the ovary in zebrafish, and a possible role in establishing/maintaining an adult stem or progenitor cell niche. Future work should focus on the migration of PGCs in embryos as well as the proliferation and apoptosis of germ cells in juveniles and young adults.

Funding

This work was supported by the NIH GM100461.

Appendix A. Supplementary data

Supplementary data to this article can be found online at https://doi.org/10.1016/j.ygcen.2019.04.003.

References

Benz, B.A., Nandadasa, S., Takeuchi, H., Takeuchi, M., Grady, R.C., LoPilato, R.K., Kakuda, S., Somerville, R.P.T., Apte, S.S., Haltiwanger, R.S., et al., 2016. Genetic and biochemical evidence that gastrulation defects in Pofut2 mutants result from defects in ADAMTS9 secretion. Dev. Biol. 416, 111–122.

Blelloch, R., Kimble, J., 1999. Control of organ shape by a secreted metalloprotease in the nematode *Caenorhabditis elegans*. Nature 399, 586–590.

Blelloch, R., Anna-Arriola, S.S., Gao, D., Li, Y., Hodgkin, J., Kimble, J., 1999. The gon-1 gene is required for gonadal morphogenesis in *Caenorhabditis elegans*. Dev. Biol. 216, 382–393.

Brown, B., Badylak, S., 2014. Extracellular matrix as an inductive scaffold for functional tissue reconstruction. Transl. Res. 163, 268–285.

Brunet, F., Fraser, F., Binder, M., Smith, A., Kintakas, C., Dancevic, C., Ward, A., McCulloch, D., 2015. The evolutionary conservation of the A disintegrin-like and metalloproteinase domain with thrombospondin-1 motif metzincins across vertebrate species and their expression in teleost zebrafish. BMC Evol. Biol. 15, 9.

Clark, M., Kelner, G., Turbeville, L., Boyer, A., Arden, K., Maki, R., 2000. ADAMTS9, a novel member of the ADAM-TS/metallospondin gene family. Genomics 67, 343–350.

Couse, J.F., Hewitt, C.S., Bunch, D.O., Sar, M., Walker, V.R., Davis, B.J., Korach, K.S., 1999. Postnatal sex reversal of the ovaries in mice lacking estrogen receptors α and β. Science 286, 2328–2331.

Deliagina, T., Wilhelm, D., Palmer, S., Pavlova, E., Koopman, P., 2002. Sex determination and gonadal development in mammals. J. Neurophysiol. 87, 1–28.

Demircan, K., Yonezawa, T., Takigawa, T., Topcu, V., Erdogan, S., Ucar, F., Armutcu, F., Yigitoglu, M.R., Ninomiya, Y., Hirohata, S., 2013. ADAMTS1, ADAMTS5, ADAMTS9 and aggrecanase-generated proteoglycan fragments are induced following spinal cord injury in mouse. Neurosci. Lett. 544, 25–30.

Dranow, D., Tucker, R., Draper, B., 2013. Germ cells are required to maintain a stable sexual phenotype in adult zebrafish. Dev. Biol. 376, 43–50.

Enomoto, H., Nelson, C.M., Somerville, R.P.T., Mielke, K., Dixon, L.J., Powell, K., Apte, S.S., 2010. Cooperation of two ADAMTS metalloproteases in closure of the mouse palate identifies a requirement for versican proteolysis in regulating palatal mesenchyme proliferation. Development (Cambridge, England) 137, 4029–4038.

Gattazzo, F., Urciuolo, A., Bonaldo, P., 2014. Extracellular matrix: a dynamic microenvironment for stem cell niche. BBA – Gen. Subj. 1840, 2506–2519.

Handbook of Proteolytic Enzymes. 2012. San Diego: Elsevier Science & Technology.

Huang, X., Hao, C., Shen, X., Zhang, Y., Liu, X., 2013. RUNX2, GPX3 and PTX3 gene expression profiling in cumulus cells are reflective oocyte/embryo competence and potentially reliable predictors of embryo developmental competence in PCOS patients. Reprod. Biol. Endocrinol. 11, 109. https://doi.org/10.1186/1477-7827-11-109.

Ismat, A., Cheshire, A.M., Andrew, D.J., 2013. The secreted AdamTS-A metalloprotease is required for collective cell migration. Development 140, 1981–1993.

Janicki, J.A., Alman, B., 2007. Scoliosis: review of diagnosis and treatment. Paediatr. Child Health 12, 771–776.

Jao, L.-E., Wente, S.R., Chen, W., 2013. Efficient multiplex biallelic zebrafish genome editing using a CRISPR nuclease system. Proc. Natl. Acad. Sci. USA 110, 13904–13909.

Jungers, K., Le Goff, C., Somerville, R., Apte, S., 2005. Adamts9 is widely expressed during mouse embryo development. Gene Expr. Patterns 5, 609–617.

Kern, C., Wessels, A., McGarity, J., Dixon, L., Alston, E., Argraves, W., Geeting, D., Nelson, C., Menick, D., Apte, S., 2010. Reduced versican cleavage due to Adamts9 haploinsufficiency is associated with cardiac and aortic anomalies. Matrix Biol. 29,

304–316.
Koo, B., Longpre, J., Somerville, R., Alexander, J., Leduc, R., Apte, S., 2006. Cell-surface processing of pro-ADAMTS9 by furin. J. Biol. Chem. 281, 12485–12494.
Liew, W., Orbán, L., 2014. Zebrafish sex: a complicated affair. Brief Funct. Genomics 13, 172–187. https://doi.org/10.1093/bfgp/elt041.
Liu, D., Brewer, M.S., Chen, S., Hong, W., Zhu, Y., 2017. Transcriptomic signatures for ovulation in vertebrates. Gen. Comp. Endocrinol. 247, 74–86. https://doi.org/10.1016/j.ygcen.2017.01.019.
Liu, D.T., Carter, N.J., Wu, X.J., Hong, W.S., Chen, S.X., Zhu, Y., 2018. Progestin and nuclear progestin receptor are essential for upregulation of metalloproteinase in zebrafish preovulatory follicles. Front. Endocrinol. (Lausanne) 9, 517. https://doi.org/10.3389/fendo.2018.00517.
McCulloch, D.R., Nelson, C.M., Dixon, L.J., Silver, D.L., Wylie, J.D., Lindner, V., Sasaki, T., Cooley, M.A., Argraves, W.S., Apte, S.S., 2009. ADAMTS metalloproteases generate active versican fragments that regulate interdigital web regression. Dev. Cell 17, 687–698. https://doi.org/10.1016/j.devcel.2009.09.008.
Meigs, J.B., Shrader, P., Sullivan, L.M., McAteer, J.B., Fox, C.S., Dupuis, J., Manning, A.K., Florez, J.C., Wilson, P.W., D'Agostino, R.B.S., et al., 2008. Genotype score in addition to common risk factors for prediction of type 2 diabetes. N. Engl. J. Med. 359, 2208–2219.
Nandadasa, S., Nelson, C., Apte, S., 2015. ADAMTS9-mediated extracellular matrix dynamics regulates umbilical cord vascular smooth muscle differentiation and rotation. Cell Rep. 11, 1519–1528. https://doi.org/10.1016/j.celrep.2015.05.005.
Orban, L., Sreenivasan, R., Olsson, P.E., 2009. Long and winding roads: testis differentiation in zebrafish. Mol. Cell. Endocrinol. 312, 35–41.
Pearson, J., Zurita, F., Tomas-Gallardo, L., Diaz-Torres, A., de la Loza, Diaz, Mdel, C., Franze, K., Martin-Bermudo, M., Gonzalez-Reyes, A., 2016. ECM-regulator timp is required for stem cell niche organization and cyst production in the drosophila ovary. PLoS Genet. 12, e1005763.
Peluffo, M.C., Murphy, M.J., Talcott Baughman, S., Stouffer, R.L., Hennebold, J.D., 2011. Systematic analysis of protease gene expression in the rhesus macaque ovulatory follicle: metalloproteinase involvement in follicle rupture. Endocrinology 152, 3963–3974.
Piprek, R., Kolasa, M., Podkowa, D., Kloc, M., Kubiak, J., 2018. Transcriptional profiling validates involvement of extracellular matrix and proteinases genes in mouse gonad development. Mech. Dev. 149, 9–19.
Ran, F.A., Hsu, P.D., Wright, J., Agarwala, V., Scott, D.A., 2013. Genome engineering using the CRISPR-Cas9 system. Nat. Protoc. 8, 2281–2308.
Rodríguez-Marí, A., Cañestro, C., Bremiller, R.A., Nguyen-Johnson, A., Asakawa, K., Kawakami, K., Postlethwait, J.H., 2010. Sex reversal in zebrafish fancl mutants is caused by Tp53-mediated germ cell apoptosis. PLoS Genet. 6, e1001034. https://doi.org/10.1371/journal.pgen.1001034.
Rosewell, K.L., Al-Alem, L., Zakerkish, F., McCord, L., Akin, J.W., Chaffin, C.L., Brannstrom, M., Curry, T.E., 2015. Induction of proteinases in the human preovulatory follicle of the menstrual cycle by human chorionic gonadotropin. Fertil. Steril. 103 (3), 826–833.
Roushandeh, A.M., Bahadori, M., Roudkenar, M.H., 2017. Mesenchymal stem cell-based therapy as a new horizon for kidney injuries. Arch. Med. Res. 48 (2), 133–146.
Santos, D., Luzio, A., Coimbra, A.M., 2017. Zebrafish sex differentiation and gonad development: a review on the impact of environmental factors. Aquat. Toxicol. 191, 141–163.
Siegfried, K.R., Nüsslein-Volhard, C., 2008. Germ line control of female sex determination in zebrafish. Dev. Biol. 324, 277–287. https://doi.org/10.1016/j.ydbio.2008.09.025.
Singleman, C., Holtzman, N.G., 2014. Growth and maturation in the zebrafish, *Danio rerio*: a staging tool for teaching and research. Zebrafish 11 (4), 396–406.
Somerville, R., Longpre, Jean-Michel, Jungers, Katherine A., Michael Engle, J., Ross, Monique, Evanko, Stephen, Wight, Thomas N., Leduc, Richard, Apte, Suneel S., 2003. Characterization of ADAMTS-9 and ADAMTS-20 as a distinct ADAMTS subfamily related to Caenorhabditis elegans GON-1. J. Biol. Chem. 278, 9503–9513.
Sun, D., Zhang, Y., Wang, C., Hua, X., Zhang, X.A., Yan, J., 2013. Sox9-related signaling controls zebrafish juvenile ovary-testis transformation. Cell Death Dis. 4, e930.
Takahashi, H., 1977. Juvenile hermaphroditism in the zebrafish, *Brachydanio rerio*. Bull. Fac. Fish. Hokkaido Univ. 18, 57–65.
Tam, C.H., Ho, J.S., Wang, Y., Lam, V.K., Lee, H.M., Jiang, G., Lau, E.S., Kong, A.P., Fan, X., Woo, J.L., et al., 2013. Use of net reclassification improvement (NRI) method confirms the utility of combined genetic risk score to predict type 2 diabetes. PLoS One 8, e83093.
Tzung, K., Goto, R., Saju, J., Sreenivasan, R., Saito, T., Arai, K., Yamaha, E., Hossain, M., Calvert, M., Orban, L., 2015. Early depletion of primordial germ cells in zebrafish promotes testis formation. Stem Cell Rep. 4, 61–73. https://doi.org/10.1016/j.stemcr.2014.10.011.
Uhlenhaut, N.H., Jakob, S., Anlag, K., Eisenberger, T., Sekido, R., Kress, J., Treier, M., Treier, A., Klugmann, C., Klasen, C., et al., 2009. Somatic sex reprogramming of adult ovaries to testes by FOXL2 ablation. Cell 139, 1130–1142.
von Hofsten, J., Olsson, P., 2005. Zebrafish sex determination and differentiation: involvement of FTZ-F1 genes. Reprod. Biol. Endocrinol. 3, 63.
Webster, K.A., Schach, U., Ordaz, A., Steinfeld, J.S., Draper, B.W., Siegfried, K.R., 2017. Dmrt1 is necessary for male sexual development in zebrafish. Dev. Biol. 422, 33–46.
Wong, T., Saito, T., Crodian, J., Collodi, P., 2011. Zebrafish germline chimeras produced by transplantation of ovarian germ cells into sterile host larvae. Biol. Reprod. 84, 1190–1197. https://doi.org/10.1095/biolreprod.110.088427.
Yoshina, S., Mitani, S., 2015. Loss of *C. elegans* GON-1, an ADAMTS9 homolog, decreases secretion resulting in altered lifespan and dauer formation. PLoS One 10, e0133966.